Hindawi Publishing Corporation
Indian Journal of Materials Science
Volume 2015, Article ID 638341, 8 pages
http://dx.doi.org/10.1155/2015/638341

Research Article

Effects of M^{2+} (M = Ca, Sr, and Ba) Addition on Crystallization and Microstructure of SiO_2-MgO-Al_2O_3-B_2O_3-K_2O-F Glass

Mrinmoy Garai, Nibedita Sasmal, and Basudeb Karmakar

Glass Science & Technology Section, Glass Division, CSIR-Central Glass & Ceramic Research Institute, 196 Raja S. C. Mullick Road, Kolkata 700032, India

Correspondence should be addressed to Mrinmoy Garai; mrinmoygarai@yahoo.in

Received 27 May 2015; Revised 23 July 2015; Accepted 26 July 2015

Academic Editor: Maximina Romero Pérez

In understanding the effect of K^+ substitution by M^{2+} (M = Ca, Sr, and Ba) on crystallization and microstructural properties of boroaluminosilicate glass system, the SiO_2-MgO-Al_2O_3-B_2O_3-MgF_2-K_2O-Li_2O-$AlPO_4$ glasses were prepared by single-step melt-quenching at 1500°C. Density of base glass (2.64 g·cm^{-3}) is found to be decreased in presence of CaO and SrO. T_g is increased by 5–10°C and T_d decreased by 13–20°C on addition of M^{2+}. The variation of T_g, T_d and decrease of thermal expansion (CTE) from 7.55 to 6.67–6.97 (×10^{-6}/K, at 50–500°C) in substituting K^+ by M^{2+} are attributed to the higher field-strength of Ca^{2+}, Sr^{2+}, and Ba^{2+}. Opaque mica glass-ceramics were derived from the transparent boroaluminosilicate glasses by controlled heat treatment at 1050°C (duration = 4 h); and the predominant crystalline phase was identified as fluorophlogopite ($KMg_3AlSi_3O_{10}F_2$) by XRD and FTIR study. Glass-ceramic microstructure reveals that the platelike mica flake crystals predominate in presence of K_2O and CaO but restructured to smaller droplet like spherical shaped mica on addition of SrO and BaO. Wide range of CTE values (9.54–13.38 × 10^{-6}/K at 50–800°C) are obtained for such glass-ceramics. Having higher CTE value after crystallization, the CaO containing SiO_2-MgO-Al_2O_3-B_2O_3-MgF_2-K_2O-Li_2O-$AlPO_4$ glass can be useful as SOFC sealing material.

1. Introduction

The development of high temperature sustainable material is an archetypal challenge to materials science researchers since the last decade. Higher thermal expansion (CTE) value and good thermal shock resistivity are two foremost criterions for this purpose. Amongst various types of high temperature materials, mica, a kind of aluminosilicate based glass-ceramic with typical layer microstructure having component system Si-Mg-Al-K-O-F, proved its effectiveness. And, thus, the increase of CTE and shock resisting capability is of great interest for mica based glass and the corresponding glass-ceramics. Over controlled heat treatment, the glass based on SiO_2-MgO-Al_2O_3-K_2O-F system is converted to glass-ceramic containing fluorophlogopite mica ($KMg_3AlSi_3O_{10}F_2$) through the process of heterogeneous phase separation, precipitation of primary crystalline nuclei, and then the formation of metastable and stable phases from these nuclei [1–3]. Different nucleating agents like ZrO_2, P_2O_5, ZnO, MnO, Fe_2O_3, Ta_2O_5, WO_3, F, and so forth are used to facilitate this crystallization mechanism [2, 3]. Due to the replacement of ions by means of similar sizes and different properties, mica phase becomes the solid solution having uncertain chemical formula. The mica crystals possess excellent cleavage planes because of the weak attraction of alkali layers. Since the progression of crystallization in silicate based glass (predominated by Si-O-Si network) considerably depends upon the nature and composition of precursor material as well as thermal treatment, the addition of different alkaline earth metal ions can affect the crystallization characteristics and microstructural properties [4–12]. In addition, the alkaline earth ion plays significant role in controlling the glass transition temperature, softening point, thermal expansion, and density of aluminosilicate glass. Of particular interest is the proportion of nonbridging oxygen (NBO), which impacts significantly on the thermal and mechanical properties. In the study of binary, ternary, and quaternary silicates of CaO, BaO, and ZnO for applying as high temperature SOFC seals, Kerstan et al. [4] established that CTE of sealing glass is affected not only by the CTE of the crystalline

Table 1: Composition (wt%) and dilatometric thermal properties of different precursor glasses.

Glass identity	K_2O[a] (wt%)	Alkaline earth[a]	Density	T_g (±1°C)	T_d (±1°C)	CTE (×10^{-6}/K) (50–500°C)
M-1	9	0	2.64	598	677	7.55
M-2	4	5 CaO	2.61	609	658	6.97
M-3	4	5 SrO	2.55	603	662	6.79
M-4	4	5 BaO	2.65	609	664	6.67

[a]Added in with base glass of 39 SiO_2-12 MgO-16 Al_2O_3-10 B_2O_3-12 MgF_2-1 Li_2O-1 $AlPO_4$ (wt%).

phases but also by that of the residual glassy phase and sealing glass's and glass-ceramic's elastic properties. Tarlakov and his coworkers [5] investigated the effects of CaO addition on the glass structure and crystallization mechanism of Li_2O-CaO-SiO_2 system. They [5] argued that the increase of CaO content in glass matrix results in increasing the temperature interval of crystallization. Hamzawy and Darwish [6] established that the substitution of Ca for Mg in stoichiometric Na-fluorophlogopite decreases the glass transformation temperature and increases the crystallization range (T_c) and thermal expansion values. They [6] furthermore accomplished that the crystallization at CaO/MgO molar ratio = 0.25 in the base glass did not enhance the formation of Na-fluorophlogopite phase but catalysed the development of fluororichterite with cristobalite crystals. In ZnO-Al_2O_3-SiO_2 based glass-ceramics, the addition of Ba^{2+} caused a structural change which renders the Si-O-Si network of the residual glassy phase in ceramic matrix more open than Ca^{2+} and Sr^{2+} [6, 7]. And the decrease in strength of glass phase network is attributed to dielectric loss. Additionally, the increase of nonbridging oxygen (O^-) and network strength (Si-O-Si) play significant role in controlling the physical and thermal properties. Yazawa and his coworkers [10] successfully prepared the alkali-resistant porous glass in SiO_2-B_2O_3-ZrO_2-RO system to ascertain the effects of MgO, CaO, SrO, BaO, and ZnO (RO). They [10] explored the effects of RO constituent to promote the phase separation in silicate based glass as CaO > SrO > BaO.

The present work is concerned to demonstrate the effect of MO (M = Ca, Sr, and Ba) addition substituting K_2O on the crystallization characteristics, microstructure, and thermal properties of Li_2O and $AlPO_4$ containing SiO_2-MgO-Al_2O_3-K_2O-B_2O_3-F (SMAKBF) glass. We report the comparative study of MO addition in SMAKBF glasses by characterizing the techniques of dilatometry, XRD, FESEM, EDX, and FTIR spectroscopy.

2. Experimental

The SMAKBF glasses were prepared from the powders of SiO_2 (Quartz Powder), Mg $(OH)_2$ (97%, Loba Chemie, Mumbai, India), Al $(OH)_3$ (97%, Loba Chemie, Mumbai, India), K_2CO_3 (98%, Loba Chemie, Mumbai, India), H_3BO_3 (99.5%, Loba Chemie, Mumbai, India), MgF_2 (99.9%, Loba Chemie, Mumbai, India), $LiCO_3$ (99.9%, Loba Chemie, Mumbai, India), $AlPO_4$ (99%, Merck, Mumbai, India), $CaCO_3$ (98%, Loba Chemie, Mumbai, India), $SrCO_3$ (98%, Loba Chemie, Mumbai, India), and $BaCO_3$ (99%, Merck, Mumbai, India) of high pure quality. The chemical compositions of the prepared glass samples are given in Table 1. Accurately weighed and homogeneously mixed (by ball milling for 1 h) batches were melted in a platinum crucible at 1500°C for 2 h. The melts were then cast into preheated graphite molds of the required dimensions. Resultant glass melts were immediately transferred into a furnace regulated at 620°C for annealing (to remove the internal stress generated during sudden cooling). Small piece of each annealed glass was then heat-treated at 1050°C (duration = 4 h) for controlled crystallization. Thermal properties such as coefficient of thermal expansion (CTE), glass transition temperature (T_g), and dilatometer softening point (T_d) were evaluated by cylinder shaped sample with length ~25 mm and diameter ~6 mm using a horizontal dilatometer, NETZSCH DIL 402 PC (NETZSCH-Gerätebau GmbH, Germany), at a heating rate of 5°C/min under ±1% accuracy after calibration with a standard Al_2O_3 cylinder. Density (d) of different glass and glass-ceramic bulk samples was determined by the Archimedes principle using distilled water as immersion liquid. The crystallization characteristics and microstructural morphology of SMAKBF glass-ceramics (heat-treated at 1050°C/4 h) were examined using field emission scanning electron microscopy (FESEM model S430i, LEO, CEA, USA) using finely polished glass-ceramic specimens (chemically etched by immersion in 2 vol% aqueous HF solution for 5 min). The crystalline phases generated in SMAKBF glass-ceramics after heat treatment (1050°C for 4 h) were identified by X-ray diffraction (XRD) analyses as recorded using a XPERTPRO MPD diffractometer (PANalytical, Almelo, Netherlands) operating with Ni-filtered CuKα = 1.5406 Å radiation as the X-ray source at voltage ~40 kV and current ~40 mA. Crystalline phases were analysed in the 2θ range 5–90° with a step size of 0.05° at room temperature (~25°C). Heat-treated SMAKBF glass-ceramics were subjected to Fourier transformed infrared (FTIR) transmission spectroscopy recorded by a FTIR spectrometer (model 1615, Perkin-Elmer Corporation, Norwalk, CT) at a resolution of ±2 cm^{-1} after 16 scans in the wave number range 400–2000 cm^{-1}. The FTIR analyses were done using the transparent thin pellet (prepared by uniaxial hydraulic press providing hand pressure ~10 tons) made by the mixture of KBr and SMAKBF glass-ceramic powder in an approximate volume proportion ~300 : 1.

3. Results and Discussion

Thermal properties, T_g, T_d, and CTE of SMAKBF glasses were evaluated by dilatometric study and represented in Figure 1.

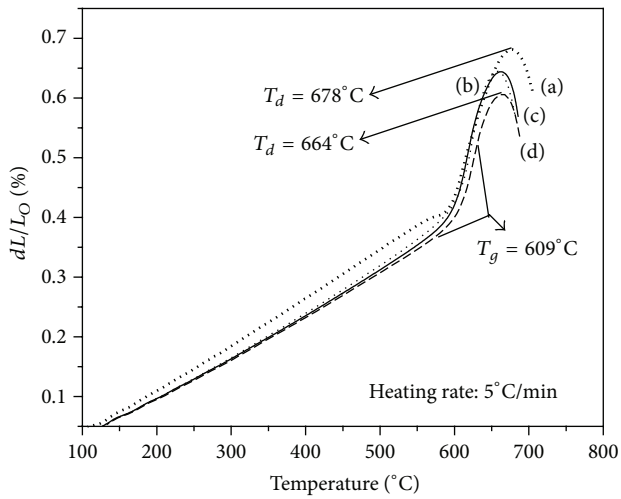

FIGURE 1: Thermal expansion behavior of precursor SiO_2-MgO-Al_2O_3-B_2O_3-K_2O-Li_2O-$AlPO_4$–F glasses.

Thermal expansion (CTE) is calculated from the elongation data and the formula is written as

$$\text{CTE} = \frac{\Delta L}{L_O} \times \frac{1}{\Delta T}, \quad (1)$$

where L_O is the initial length and ΔL and ΔT are the difference in length and temperature of sample, respectively. For glassy material, thermal expansion value is increased with temperature and at glass transition point it increases very much due to considerable decrease in viscosity. As evident from Figure 1, the linear increase in CTE up to T_g followed by sudden jump and then decrease after T_d is displayed by all the SMAKBF glasses. For M-1 glass, the CTE value is evaluated as 7.11 and 7.55 × 10^{-6}/K at 50–300 and 50–500°C, respectively. As seen from Table 1, CTE value decreased to 6.67–6.97 × 10^{-6}/K at 50–500°C on addition of MO (M is Ca, Sr, and Ba) in place of K_2O (5 wt%). The decrease in CTE can be attributed to the cationic field strength $[z_i/(r_R + r_O)^2$, where z_i, r_R, and r_O are the charge of cation, radius of cation, and radius of anion, resp.] of the additive alkaline earth metals. When M^{2+} (M = Ca/Sr/Ba) having larger field strength (Ca^{2+} = 0.35, Sr^{2+} = 0.32, and Ba^{2+} = 0.27) than K^+ (0.13) is added in the SiO_2-MgO-Al_2O_3-K_2O-B_2O_3-Li_2O-$AlPO_4$-F glass system, the strength of glass structure (controlled by Si-O-Si network) is increased, and, hence, thermal expansion value decreased. Density of M-1 glass is calculated as 2.64 g·cm^{-3}. As seen from Table 1, T_g and T_d value of the SMAKBF glass are varied considerably on substituting K^+ by Ca^{2+}, Sr^{2+}, and Ba^{2+}. M-1 glass, containing 12 wt% MgO and 9 wt% K_2O, possesses T_g value 598°C. It is increased to 609, 603, and 609°C on addition of CaO, SrO, and BaO, respectively. In M-1 system, total glass modifier oxide content is 22 wt% (12 MgO + 9 K_2O + 1 Li_2O), where the alumina content is 16 wt% (16 Al_2O_3) and B_2O_3 = 10 wt%. When the total of Al_2O_3 and B_2O_3 content is almost balanced by modifier oxide, the all O atoms are in bridging approach, that is, Al-O-Al and B-O-B along with Si-O-Si. The addition of modifier oxide results in increase of nonbridging oxygen (NBO), which affects the stabilization of glass matrix to increase the glass transition range. After T_g point, the structural relaxation occurring in Si-O-Si glass matrix caused the increase of CTE value exceedingly up to T_d temperature. For M-1 glass, CTE value obtained at 50–700°C is 9.66 × 10^{-6}/K and decreased on addition of MO. T_d value obtained for M-1 glass is 677°C and decreased to 658, 662, and 664°C for M-2, M-3, and M-4 glasses, respectively, due to the decrease of electrostatic attraction. Potassium (K^+), being the network modifier ion, binds together with silicate anions (SiO_4^{4-}) by electrostatic force of attraction and hence effectively acts as ionic bridges between two kinds of nonbridging oxygen (NBO). The addition of CaO, SrO, and BaO replacing K_2O results in reducing the electrostatic forces between the kinds of nonbridging oxygen (NBO) considerably and hence decreases the T_d value of glasses [12]. Likewise T_d, density of M-2 (CaO content) and M-3 (SrO content) glass is reduced and evaluated as 2.61 and 2.55 g·cm^{-3}, respectively. It is somewhat increased on addition of BaO because of large atomic mass compared to CaO and SrO, because the cation size of Ba^{2+} is 33% larger than Ca^{2+}, but mass of BaO (molecular weight = 153 g) is almost 3.4 times larger than CaO (molecular weight = 56 g).

The crystallization characteristics of SMAKBF glasses have been intended by XRD technique in the 2θ range of 5–90°. The hump that appeared at around (2θ) 20–35° in Figure 2 confirms the amorphous nature of the present SiO_2-MgO-Al_2O_3-B_2O_3-MgF_2-K_2O-Li_2O-$AlPO_4$ glasses. The transparent SMAKBF glasses were crystallized at 1050°C (for 4 h duration) to convert into opaque glass-ceramic (GC). The crystalline nature of four synthesized glasses is represented in Figure 3. As is evident from Figure 3, the two higher intense crystalline planes (001) and (003) are formed at 2θ = 8.82 and 26.72° for all the glass-ceramics. In addition, three low intense crystalline planes (200), (005), and (331) are developed due to phase reflections at 2θ = 34.14, 45.50, and 60.34°. All these crystalline planes appeared due to the formation of crystalline phase fluorophlogopite mica, $KMg_3AlSi_3O_{10}F_2$ (monoclinic end centered system, JCPDS file number 10-0494, molecular weight = 421.24, lattice parameter a = 5.299, b = 9.188, and c = 10.13), where the tightly bonded aluminosilicate sheets $[Mg_3(AlSi_3O_{10})F_2]^-$ are weakly bonded together by large 12-coordinated K^+ ions [12]. In presence of CaO, SrO, and BaO, crystalline peak intensity is increased (as seen from Figure 3) due to favorable crystallization owing to the large cationic field strength (cluster forming tendency). Two additional phase reflections at 28.25 and 30.87 (2θ) corresponding to (112) and (113) planes are observed for M-3 and M-4 glass-ceramics (Figure 3(c) and (d)). Development of this fluorophlogopite mica is composed of some crucial stages like amorphous phase separation, precipitation of primary crystalline nuclei, and the formation of metastable and stable phases from these nuclei [1, 2]. The primary nucleation phenomenon of SiO_2-MgO-Al_2O_3-B_2O_3-MgF_2-K_2O-Li_2O-$AlPO_4$ glass is supposed to be the precipitation of F- and

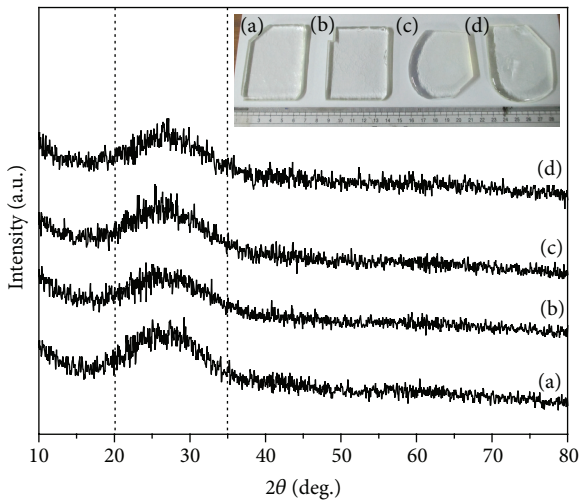

Figure 2: X-ray diffractogram of precursor (a) M-1, (b) M-2, (c) M-3, and (d) M-4 glasses (inset shows the photograph of transparent SiO_2-MgO-Al_2O_3-B_2O_3-K_2O-Li_2O-$AlPO_4$–F glasses synthesized by melt quenching).

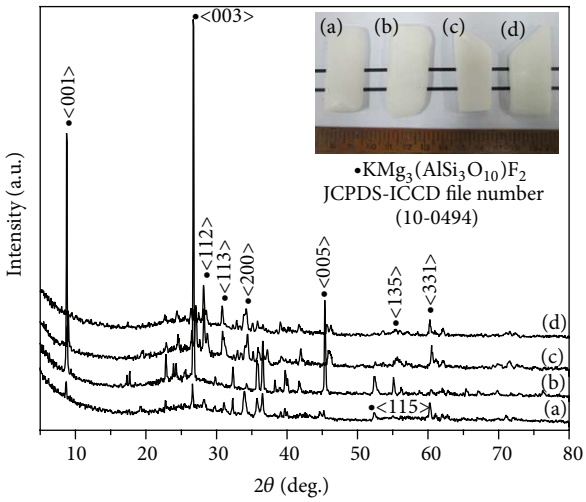

Figure 3: XRD analysis of M-1 (a), M-2 (b), M-3 (c), and M-4 (d) glass-ceramics heat-treated at 1050°C for 4 h (inset shows the photograph of opaque glass-ceramics developed from SiO_2-MgO-Al_2O_3-B_2O_3-K_2O-Li_2O-$AlPO_4$–F glasses).

Mg-rich phase MgF_2 on heating above annealing temperature (620°C). Ca^{2+}, Sr^{2+}, and Ba^{2+} having larger cationic field strength can form "cluster" to initiate heterogeneous phase separation. During the primary stage of crystallization event, very fine grained crystals of norbergite (Mg_2SiO_4·MgF_2), MgF_2, and mullite ($3Al_2O_3$·$2SiO_2$) are developed [1, 2, 12, 13]. Further heating results in increasing the crystallization of mullite phase. And then a typical solid phase reaction of norbergite and mullite crystals with K_2O-SiO_2 glass takes place which finally results in producing two-dimensional fluorophlogopite mica crystalline phase. Increase in the quantity of mica crystals occurs on further heating and, at 1050°C, the randomly distributed mica crystal predominates in the ceramic matrix [12].

Thermal, optical, and mechanical properties are significantly changed when silicate based glass materials are converted into glass-ceramics. Amount, variety, shape, and packing of the crystalline phases developed in glass-ceramic matrix contribute significantly on the variation of these properties. In order to ascertain the change in microstructural morphology on substituting K^+ by Ca^{2+}, Sr^{2+}, and Ba^{2+}, the field emission scanning electron microscopy (FESEM) was done for SMAKBF glass-ceramics heat-treated at 1050°C. SMAKBF glasses are converted to glass-ceramics containing fluorophlogopite mica, $KMg_3(AlSi_3O_{10})F_2$ crystalline phases predominately, which are mainly responsible for varying the thermal properties of present glass-ceramics. In Figure 4, the FESEM morphology of glass-ceramics (GC) heat-treated at 1050°C for 4 h is represented. Microstructure of the M-1 GC is exhibited in Figure 4(a), whereas Figures 4(b)–4(d) depict the microstructure of CaO, SrO, and BaO (5 wt%) containing GCs, respectively. As is evident from Figure 4(a), M-1 GC is composed of some rodlike cylindrical shaped and some platelike fluorophlogopite mica [$KMg_3(AlSi_3O_{10})F_2$] flake crystals randomly dispersed throughout the crystallized matrix. It possesses density value 2.66 g·cm^{-3} and thermal expansion (CTE) 8.69 and 13.38 × 10^{-6}/K at 50–500 and 50–800°C, respectively. Alkali quantity (K_2O) in M-1 glass is 9 wt%. As seen from Figure 4(b), 5 wt% CaO/K_2O substitution results in the crystalline aggregation of smaller mica crystals, to develop longer platelike microstructure and, hence, homogeneous compactness. This compactness of microstructure caused its thermal expansion values to be reduced into 7.20 and 12.68 × 10^{-6}/K at 50–500 and 50–800°C, respectively. Density of M-2 GC is calculated as 2.63 g-cm^{-3}. The CaO has a bit tendency to substitute some K_2O in the chemical formula of mica, $K(Mg,Ca)_3AlSi_3O_{10}F_2$. Mica belongs to the end centered cubic lattice and monoclinic system where several kinds of atoms can coexist. Thus, uniform nucleation is difficult to occur in the glass phase on heat treatment. In Figure 4(c), the microstructure of M-3 GC where 5 wt% K_2O has been substituted by SrO is represented. There, the platelike mica crystals are broken into smaller droplet like micas and the droplet like mica crystals are agglomerated for endowing a compact microstructure. A large number of spherical particles, which are almost uniform in size (average particle diameter is about 200–400 nm), coexist there. Therefore, the thermal expansion value is reduced to 7.56 and 9.54 × 10^{-6}/K at 50–500 and 50–800°C, respectively. Figure 4(d) depicts the microstructure of M-4 GC, where 5 wt% K_2O is substituted by BaO. This microstructure is exceedingly different from others; 2–6 μm sized cylindrical shaped fluorophlogopite mica crystals are predominating in the matrix. Better fitted arrangement with mica crystals in this GC is responsible for higher density (2.68 g-cm^{-3}) and lower thermal expansion value. At 50–500 and 50–800°C, CTE of M-4 GC is 7.23 and 10.91 × 10^{-6}/K, respectively. Higher thermal expansion value (10.91–13.38 × 10^{-6}/K) of M-1, M-2, and M-4 glass-ceramic makes them useful for high temperature vacuum sealing application with metal having higher thermal expansion coefficient.

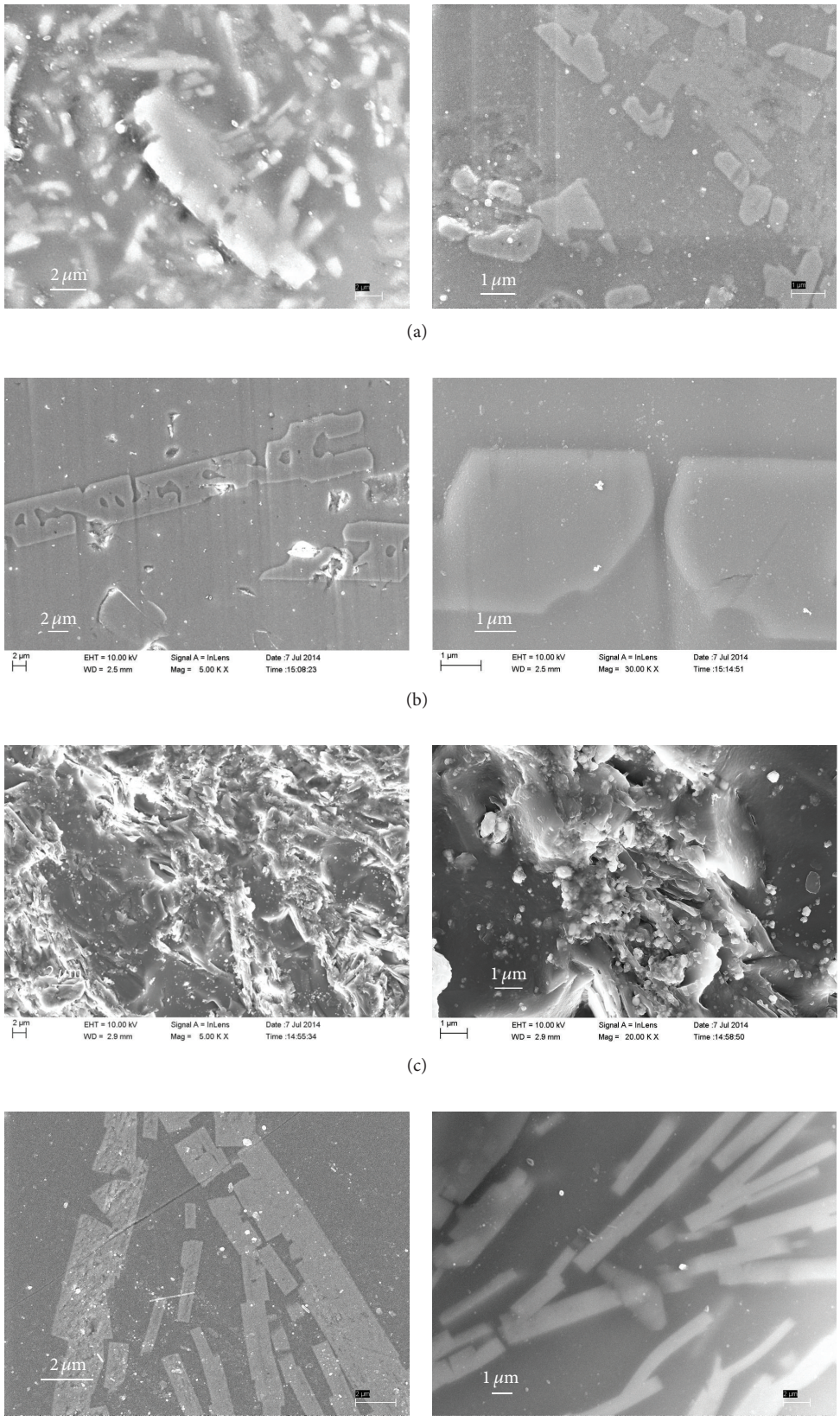

Figure 4: FESEM photomicrograph of (a) M-1, (b) M-2, (c) M-3, and (d) M-4 glass-ceramic specimens (chemically etched by immersion in 2 vol% aqueous HF solution for 5 minutes) heat-treated at 1050°C for 4 h.

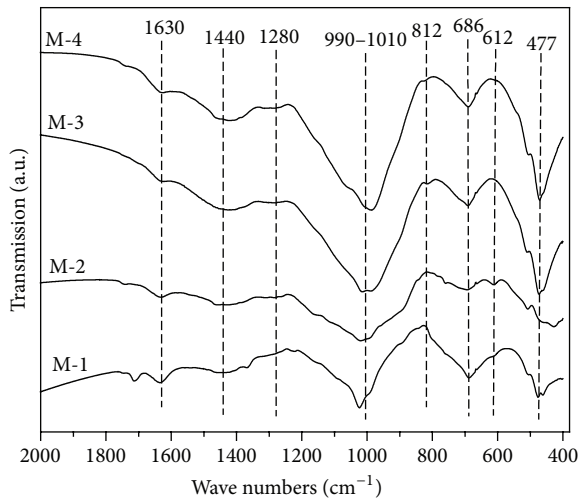

Figure 5: FTIR transmission spectra of glass-ceramics heat-treated at 1050°C for 4 h (see Table 2 for IR band assignments).

Table 2: FTIR band position and assignment of different glass-ceramics heat-treated at 1050°C/4 h.

Band position (cm^{-1})	Band assignment
477	Si-O-Si bending vibration modes of [SiO_4] unit
612	Al-O-Al stretching vibration of [AlO_6] unit
686	Si-O-Si symmetric stretching vibration of [SiO_4] unit
812	Si-OH stretching vibration mode
990–1010	Si-O-Si asymmetric stretching vibration B-O stretching vibration of [BO_4] units
1280	Antisymmetric stretching vibration of Si-O-Si of [SiO_4] unit
1440	B-O symmetric stretching vibration related to tri-, tetra-, and pentaborate groups
1630	H-O-H bending vibration of molecular water

In Figure 5, the FTIR transmission spectra of SMAKBF glass-ceramics (GCs) are depicted in the wave number range of 400–2000 cm^{-1}. The different bands appeared in Figure 5 and respective wave numbers are almost the same for all the SMAKBF GCs. Table 2 provides the different transmission bands and their respective band assignments. The transmission band centered at 477 cm^{-1} for all the GCs corresponds to Si-O-Si bending vibration for tetrahedral [SiO_4] unit [14–20]. Initial substitution of CaO in place of K_2O strengthens the Si-O-Si network and hence glass structure. The addition of modifier oxide results in increase of nonbridging oxygen (NBO), which affects the stabilization of glass matrix controlled by Si-O-Si network. Higher ionic radius of Sr^{2+} and Ba^{2+} further decreased their cationic field strength, and so higher intense band appeared at 477 cm^{-1} for M-3 and M-4 GCs compared to M-1 and M-2. The transmission band at 612 cm^{-1} for M-2 GC is assigned to Al-O-Al stretching vibration of octahedral [AlO_6] units [20, 21]. And the band peak position at 686 cm^{-1} is ascribed to Al-O-Al symmetric stretching vibration of 4-coordinated [AlO_4] unit [16–18]. Here, an interesting observation is the disappearance of the band at 612 cm^{-1} in M-3 and M-4 GCs. When 5 wt% K_2O (of M-1 system) is substituted by CaO, octahedral [AlO_6] units are developed. But the substitution by SrO and BaO results in converting the 6-coordinated [AlO_6] units into 4-coordinated [AlO_4] units due to higher atomic volume of Sr and Ba. The FTIR spectrum for all four GCs illustrates a characteristic band region at 990–1010 cm^{-1} which corresponds to Si-O-Si asymmetric stretching vibration of SiO_4 unit [14–18]. The band region is broadened due to the B-O stretching vibration of 4-coordinated [BO_4] units which has also characteristic band at this region of 990–1010 cm^{-1}. The sharp band at this wave number (990–1010 cm^{-1}) for all the systems suggests that the glass structure is predominately controlled by silicate (SiO_4) network and the addition of larger alkaline earth ion does not affect the network vibration considerably. In all the four SMAKBF GCs, the lower intense transmission band at 1280 cm^{-1} is attributed to Si-O-Si antisymmetric stretching vibration of [SiO_4] unit. Another low intense band region at 1440 cm^{-1} is assigned to B-O symmetric stretching vibration of tetrahedral [BO_4] units. In the spectrum of all investigated SMAKBF GCs, the characteristic band at 1630 cm^{-1} is due to H-O-H bending vibration of H_2O molecule [21, 22].

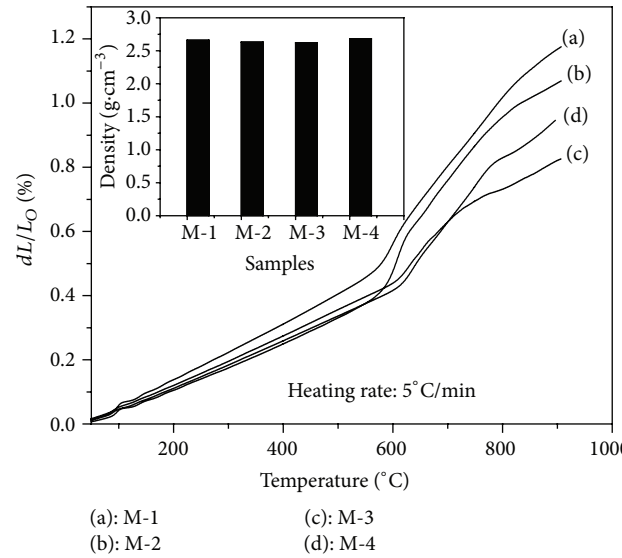

Figure 6: Comparison of thermal expansion trend as a function of temperature of GCs heat-treated at 1050°C for 4 h (see Table 3 for detailed CTE values and inset shows the variation of density of glass-ceramics).

In Figure 6, the CTE trend of all SMAKBF GCs (heat-treated at 1050°C) is represented. The linear increase of CTE is seen for each SMAKBF GC although its value is decreased on addition of CaO, SrO, and BaO. Table 3 provides

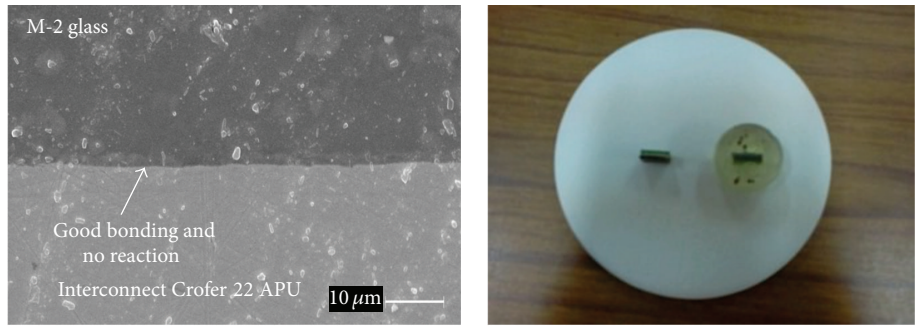

(a) (b)

Figure 7: (a) FESEM photograph of glass to SOFC interconnect interface (with 10-micron scale bar) showing good bonding without any chemical reaction and (b) coupon cells prepared using YSZ electrolyte and M-2 glass seal.

Table 3: Variation of CTE of different glass-ceramics heat-treated at 1050°C for 4 h.

Sample identity	Coefficient of thermal expansion ($\times 10^{-6}$/K)				
	50–300°C	50–500°C	50–700°C	50–800°C	50–900°C
M-1	8.35	8.69	12.15	13.38	13.57
M-2	6.71	7.20	11.58	12.66	12.42
M-3	7.16	7.56	9.43	9.54	9.47
M-4	6.89	7.23	9.51	10.91	11.05

the CTE values in the temperature range of 50–300, 50–500, 50–700, 50–800, and 50–900°C. For mica based glass-ceramic materials, the thermal expansion is significantly dependent on nature and amount of crystalline phases and also microstructural arrangement. M-1 as prepared glass possesses thermal expansion value 7.11×10^{-6}/K at 50–300°C. After heating at 1050°C, it is converted to glass-ceramic containing fluorophlogopite mica and so the CTE is increased to 8.35×10^{-6}/K. With increasing the alkaline earth metal content (in place of K_2O) in M-1 glass-ceramic, CTE value decreased due to the higher cationic field strength of M^{2+} ions. In SMAKBF system, the accumulation of glass modifier oxide results in increase of nonbridging oxygen (NBO), which affects the stabilization of glass-ceramic matrix to increase the thermal expansion value. CTEs obtained for M-2, M-3, and M-4 GCs are 6.71, 7.16, and 6.89 ($\times 10^{-6}$/K), respectively, at 50–300°C (Table 3). In the temperature range 50–800°C, CTEs of M-1, M-2, M-3, and M-4 GCs are 13.38, 12.66, 9.54, and 10.91×10^{-6}/K, respectively, which are higher due to the presence of fluorophlogopite mica. In the temperature range 50–900°C, CTE values are 9.47–13.57×10^{-6}/K, and this wide variation can be attributed to the change in microstructural morphology. As seen from Figure 4(c), the compact interlocked type microstructure is developed in SrO containing GC and this is the reason of its lower CTE value. Higher thermal expansion (12.42–13.57×10^{-6}/K at 50–900°C) of these (M-1 and M-2) GCs makes them efficiently useful for high temperature vacuum sealing application with metal. And the linear increase of CTE, obtained up to 900°C for SMAKBF GCs, indicates that these glasses are not liable for crack generation in a thermal recycling operation for high temperature application purpose (like SOFC). Figure 7 confirms the effectiveness of M-2 glass (CaO content = 5 wt%) as a good sealing material for solid oxide fuel cell (SOFC), as it has not fashioned any chemical reaction with SOFC interconnect material, Crofer 22 APU. The glass seal was not liable to any considerable chemical reaction with SOFC electrolyte, yttria stabilized zirconia (YSZ).

4. Conclusions

In this study, 5 wt% K_2O of $39SiO_2$-$12MgO$-$16Al_2O_3$-$10B_2O_3$-$12MgF_2$-$9K_2O$-$1Li_2O$-$1AlPO_4$ (wt%) glass is substituted by CaO, SrO, and BaO and the relevant alteration of thermal properties, crystallization pattern, and microstructure have been inspected to draw the following conclusions:

(i) The glass transition temperature (T_g) is increased and dilatometric softening point (T_d) decreased on addition of CaO, SrO, and BaO substituting K_2O (5 wt%).

(ii) Transparent boroaluminosilicate glasses are converted into opaque glass-ceramics on controlled heat treatment at 1050°C and the predominant crystalline phase is identified as fluorophlogopite mica, $KMg_3AlSi_3O_{10}F_2$. The platelike fluorophlogopite mica flake crystals predominate in presence of K_2O and CaO but changed to smaller droplet like spherical shaped mica on addition of SrO and BaO. CaO containing boroaluminosilicate glass seal provides good bonding with solid oxide fuel cell materials without any considerable reaction.

(iii) Density trend of glasses and glass-ceramics increases in direction of BaO addition > base glass > CaO addition > SrO addition.

(iv) Thermal expansion coefficients of precursor boroaluminosilicate glass samples in temperature range 50–500°C changed from 7.55×10^{-6}/K to 6.67–6.97×10^{-6}/K in presence of CaO, SrO, and BaO. For glass-ceramics, a wide range of thermal expansion values (9.54–13.38×10^{-6}/K at 50–800°C) are obtained.

The higher value of thermal expansion coefficients of CaO and BaO containing glass-ceramics makes them appropriate for high temperature vacuum sealing application with metal possessing large thermal expansion.

Conflict of Interests

The authors declare that there is no conflict of interests regarding the publication of this paper.

Acknowledgments

The authors thank Mr. Kamal Dasgupta, Acting Director, Dr. R. Sen, Head, Glass Division, and Dr. R. N. Basu, Head, Fuel Cell and Battery Division, for their encouragement and support to carry out this work. They thankfully acknowledge the CSIR-NMITLI funded project TLP 0005 for financial support. They are thankful to Dr. K. Annapurna for FTIR study, XRD and Electron Microscope Sections of this institute.

References

[1] D. G. Grossman, "Machinable glass-ceramics based on tetrasilicic mica," *Journal of the American Ceramic Society*, vol. 55, no. 9, pp. 446–449, 1972.

[2] W. Höland and G. H. Beall, *Glass-Ceramic Technology*, The American Ceramic Society, Westerville, Ohio, USA, 2002.

[3] H.-I. Hsiang, S. W. Yung, and C. C. Wang, "Crystallization, densification and dielectric properties of CaO-MgO-Al_2O_3-SiO_2 glass with ZrO_2 as nucleating agent," *Materials Research Bulletin*, vol. 60, pp. 730–737, 2014.

[4] M. Kerstan, M. Müller, and C. Rüssel, "Binary, ternary and quaternary silicates of CaO, BaO and ZnO in high thermal expansion seals for solid oxide fuel cells studied by high-temperature X-ray diffraction (HT-XRD)," *Materials Research Bulletin*, vol. 46, no. 12, pp. 2456–2463, 2011.

[5] Y. P. Tarlakov, I. F. Es'kova, and A. M. Shevyakov, "Spectroscopic study of high silica glasses of the lithium oxide-sodium oxide-calcium oxide-silicon dioxide system," *Issled. Strukt. Sostyaniya Neorg. Veshchestu*, vol. 1, pp. 7–10, 1974.

[6] E. M. A. Hamzawy and H. Darwish, "Crystallization of sodium fluormica Na(Mg, Zn, Ca)$_{2.5}Si_4O_{10}F_2$ glasses," *Materials Chemistry and Physics*, vol. 71, no. 1, pp. 70–75, 2001.

[7] S. N. Hoda and G. H. Beall, "Advances in ceramics," *Journal of the American Ceramic Society*, vol. 54, p. 287, 1982.

[8] C. B. da Silveira, S. D. de Campos, S. C. de Castro, and Y. Kawano, "Preparation and characterization of glass-ceramic materials in the BaO-Li_2O-ZrO_2-SiO_2 system and their dependence on treatment temperatures," *Materials Research Bulletin*, vol. 34, no. 10, pp. 1661–1671, 1999.

[9] P. W. McMillan and G. Partridge, "The dielectric properties of certain ZnO-Al_2O_3-SiO_2 glass-ceramics," *Journal of Materials Science*, vol. 7, no. 8, pp. 847–855, 1972.

[10] T. Yazawa, H. Tanaka, K. Eguchi, and S. Yokoyama, "Novel alkali-resistant porous glass prepared from a mother glass based on the SiO_2-B_2O_3-RO-ZrO_2 (R = Mg, Ca, Sr, Ba and Zn) system," *Journal of Materials Science*, vol. 29, no. 13, pp. 3433–3440, 1994.

[11] X.-M. Qin, X.-Y. Sun, Z.-M. Xiu, and L. Zuo, "Effects of ZrO_2 on the microstructure of a mica glass-ceramic," *Chinese Journal of Structural Chemistry*, vol. 23, no. 10, pp. 1111–1116, 2004.

[12] M. Garai, N. Sasmal, A. R. Molla, S. P. Singh, A. Tarafder, and B. Karmakar, "Effects of nucleating agents on crystallization and microstructure of fluorophlogopite mica-containing glass-ceramics," *Journal of Materials Science*, vol. 49, no. 4, pp. 1612–1623, 2014.

[13] E. Ercenk and S. Yilmaz, "Crystallization kinetics of mica glass-ceramic in the SiO_2-Al_2O_3-MgO-K_2O-B_2O_3-F_2 system," *Journal of Ceramic Processing Research*, vol. 16, pp. 169–175, 2015.

[14] G. Kaur, M. Kumar, A. Arora, O. P. Pandey, and K. Singh, "Influence of Y_2O_3 on structural and optical properties of SiO_2–BaO–ZnO–xB_2O_3–(10–x) Y_2O_3 glasses and glass ceramics," *Journal of Non-Crystalline Solids*, vol. 357, no. 3, pp. 858–863, 2011.

[15] M. Garai, N. Sasmal, A. R. Molla, and B. Karmakar, "Structural effects of Zn^{+2}/Mg^{+2} ratios on crystallization characteristics and microstructure of fluorophlogopite mica-containing glass-ceramics," *Solid State Sciences*, vol. 44, pp. 10–21, 2015.

[16] G. Fuxi, *Optical and Spectroscopic Properties of Glass*, Springer, Berlin, Germany, 1992.

[17] S. G. Motke, S. P. Yawale, and S. S. Yawale, "Infrared spectra of zinc doped lead borate glasses," *Bulletin of Materials Science*, vol. 25, no. 1, pp. 75–78, 2002.

[18] S. P. Singh, K. Pal, A. Tarafder, M. Das, K. Annapurna, and B. Karmakar, "Effects of SiO_2 and TiO_2 fillers on thermal and dielectric properties of eco-friendly bismuth glass microcomposites of plasma display panels," *Bulletin of Materials Science*, vol. 33, no. 1, pp. 33–41, 2010.

[19] J. Yu, X. Zhao, J. C. Yu, G. Zhong, J. Han, and Q. Zhao, "The grain size and surface hydroxyl content of super-hydrophilic TiO_2/SiO_2 composite nanometer thin films," *Journal of Materials Science Letters*, vol. 20, no. 18, pp. 1745–1748, 2001.

[20] P. Tarte, "Infra-red spectra of inorganic aluminates and characteristic vibrational frequencies of AlO_4 tetrahedra and AlO_6 octahedra," *Spectrochimica Acta Part A: Molecular Spectroscopy*, vol. 23, no. 7, pp. 2127–2143, 1967.

[21] M. Garai, N. Sasmal, A. R. Molla, A. Tarafder, and B. Karmakar, "Effects of in-situ generated coinage nanometals on crystallization and microstructure of fluorophlogopite mica containing glass-ceramics," *Journal of Materials Science & Technology*, vol. 31, no. 1, pp. 110–119, 2015.

[22] N. Abd El-Shafi and M. M. Morsi, "Optical absorption and infrared studies of some silicate glasses containing titanium," *Journal of Materials Science*, vol. 32, no. 19, pp. 5185–5189, 1997.